Adsorption and desorption of a wetting fluid in Vycor studied by acoustic and optical techniques

J. H. Page,[1] J. Liu,[2] B. Abeles,[3] E. Herbolzheimer,[3] H. W. Deckman,[3] and D. A. Weitz[3]
[1]*Department of Physics, University of Manitoba, Winnipeg, Manitoba, Canada R3T 2N2*
[2]*Department of Physics, California State University at Long Beach, Long Beach, California 90840*
[3]*Exxon Research and Engineering Company, Route 22E, Annandale, New Jersey 08801*
(Received 15 September 1994; revised manuscript received 6 April 1995)

We study the adsorption and desorption of hexane in porous Vycor, as the ambient vapor pressure is varied, through sorption isotherm, ultrasonic velocity and attenuation, and light scattering measurements. On adsorption, we show that the fluid fills the pore space uniformly until capillary condensation occurs; however, small, randomly distributed, vapor bubbles remain, as detected by a large increase in the attenuation of the ultrasound. On desorption, the mismatch in the index of refraction between the empty pores and the surrounding filled pores leads to intense scattering of light that reveals the presence of long-range correlations in the pore space. These correlations have a fractal dimension of 2.6, which is very near the value predicted for invasion percolation. Finally, we also investigate the time dependence of the changes in the adsorbed fluid mass and use these measurements to identify three distinct regimes with vastly differing mechanisms for mass transport. The results presented here provide information on the differences in pore-space correlations on filling and drainage, and highlight the critical role of the connectivity of the pores to the surface in determining the desorption behavior.

PACS number(s): 68.45.Da, 61.43.Hv, 68.10.Jy, 68.45.Nj

I. INTRODUCTION

The interaction of fluids with porous materials is significantly different from that with smooth interfaces [1,2]. Both the adsorption of the fluid as the pressure of the ambient vapor is increased and the desorption as the pressure is decreased are dramatically modified. On adsorption, the large surface area per unit volume of a porous material leads to a correspondingly large increase in the amount of fluid that can be interfacially adsorbed at low pressures of the ambient vapor. At higher pressures, the small pores result in capillary condensation of the fluid, causing a significantly larger amount of fluid to be adsorbed at pressures well below the saturation vapor pressure. On desorption of fluid from a completely saturated porous material, the random structure of the pore space plays a critical role, limiting the connectivity of filled pores to the ambient vapor as its pressure is decreased, causing highly disordered pathways of empty pores as they drain.

A fundamental understanding of the interactions of porous materials with fluids has vast practical importance [1,2]. Porous materials are crucial to a wide range of technologies, such as catalyst supports and ultrafiltration membranes, and the adsorption and desorption of fluids are critical in their performance. In particular, the behavior on fluid adsorption and desorption is often used to characterize the pore space of the material and to determine the distribution of pore sizes. This is accomplished through a sorption isotherm, in which the amount of fluid adsorbed in the porous material is measured as the pressure of the ambient vapor is increased and then decreased. The basis for this methodology is the pronounced change in the saturation pressure of the ambient vapor for a small pore, due to capillary condensation of the fluid, and the strong dependence of this saturation pressure on the radius of the pore, as described by the Kelvin equation [2]. The reduction in the amount of fluid in the porous material as the ambient pressure is reduced is usually interpreted to yield a measure of the pore size distribution [1]. However, essential to this interpretation is the assumption that all pores are fully connected to the surface and the ambient vapor, so that the Kelvin equation can be used to determine the pore size distribution. If this connectivity is not established, all the traditional interpretations of the pore size measurements are highly dubious, and the whole methodology must be reexamined [3]. The key to testing the validity of these measurements is determining the correlations in the empty pores as they drain [4]. If all the pores of a given size empty at a given pressure, as is assumed, then the empty pores should be randomly situated as they drain, and there should be no correlations between them. By contrast, if the random geometry restricts the connectivity of the pores to the surface, the empty pores should exhibit long-range correlations as the fluid is drained. Thus, a detailed investigation of the behavior of a porous material on desorption of the fluid as the pressure of the ambient vapor is reduced is essential to test the validity of these characterization techniques.

The adsorption behavior of a porous material on filling with fluid is very different, but also very interesting and important. The critical behavior is determined by the capillary condensation of the fluid to saturate the pores fully. The geometry of the fluid as it fills the pore space is thus markedly different from the case of drainage. Therefore, the connectivity to the surface is also expected to be different, and thus the possibility of long-range correlations is greatly reduced. Nevertheless, recent theoretical

work [5] has suggested that the filling of a porous material with fluid should not proceed completely uniformly but should result in the formation of bubbles of vapor in the fluid before it is completely filled. A careful investigation of the behavior of a porous material as fluid is adsorbed into the pores is required to test this assertion.

Vycor has long served as a prototypic porous material [6,7]. The pore space in this borosilicate glass is formed by a process of spinodal decomposition of a boron-rich phase, which is then chemically etched out. This results in a random, interconnected pore space, occupying about 30% of the total volume. The pores are roughly 30 Å in radius, separated by about 190 Å, and have a short-range correlation in position characteristic of a material formed through spinodal decomposition. Vycor is a very important material for technology, as it serves as the precursor for the formation of many modern glassware products. In addition, the high degree of uniformity, the small size, and the large volume of its pores has made Vycor ideal for studying the behavior of fluids within porous materials.

In this paper, we present the results of a study of the adsorption and desorption of hexane in Vycor. We combine two independent experimental techniques, ultrasonic propagation and light scattering, to elucidate the behavior. We use ultrasonic measurements to probe the nature of the fluid as it is adsorbed in the pore space. The transit velocity of ultrasonic pulses provides a very sensitive measure of the amount of fluid adsorbed in the pore space; it also probes the small changes in the rigidity of the Vycor itself as the pores are filled with fluid. The ultrasonic attenuation probes the structure of inhomogeneities in the pore space as it is emptied or filled. The light scattering measurements directly probe the long-range correlations that are produced as the fluid is drained from the Vycor.

We show that the correlations in the partially filled pore space are dramatically different on filling than on draining. On filling, we find no long-range correlations in the filled pores; instead we find that the pore walls are initially coated uniformly with fluid until the pressure is sufficiently large for capillary condensation to occur, whereupon randomly distributed bubbles of vapor are formed in the larger pores as the smaller pores become completely filled. These uncorrelated vapor bubbles shrink as the pressure is increased further, but are not eliminated until all the pores are completely filled. These bubbles lead to a marked increase in the ultrasonic attenuation. On draining, we observe extended fractal correlations of the drained pores, with a fractal dimension of $d_f \approx 2.6$, consistent with the value expected for the analogous process of invasion percolation [8–11].

We also investigate the time evolution of the change in the hexane absorption when the Vycor is subjected to a step change in the pressure. From this, we extract the diffusion coefficient of the hexane in Vycor; it is markedly different depending on whether the transport process is the relatively slow surface diffusion of interfacially adsorbed hexane or the much more rapid diffusion of changes in the liquid hexane density once capillary condensation of the fluid has completely filled the pores. At the point where the critical light scattering occurs, the hexane desorption also exhibits a nonuniform behavior and a large susceptibility to fluctuations, consistent with the behavior expected near a critical point. The combination of all these results provides a consistent picture for the dynamics and structures formed when a single fluid and its vapor coexist in a porous medium.

The paper is divided as follows: In Sec. II, we present a description of both the ultrasonic and the light scattering experiments. This is followed by a more detailed discussion of the sorption isotherms of Vycor in Sec. III. We then present details of the behavior of the Vycor on adsorption in Sec. IV, followed by the behavior on desorption in Sec. V. A discussion of the analysis of the time dependence of the fluid and vapor flow in the Vycor follows in Sec. VI. Section VII summarizes our most important results and conclusions.

II. EXPERIMENT

A. Ultrasonic measurements

The ultrasonic experiments were performed on a Vycor rod, of diameter $d=7.0$ mm and length $L=3.8$ cm. The ends of the sample were cut with a diamond saw and then polished flat and parallel with aluminum oxide lapping film. Ultrasonic transmission measurements were performed by pressing the Vycor sample between two identical fused quartz delay rods, on the opposite ends of which were bonded lead metaniobate transducers. The transducers and delay rods were both 0.5 in. in diameter. Porous, compressible Teflon films, nominally 25 μm thick, were used to couple the ultrasonic energy across the interfaces between the sample and the quartz delay rods; this material was chosen over more conventional ultrasonic bonding agents since, unlike silicone fluids and epoxies, it could not contaminate the porous Vycor sample by being sucked into the pores and it would neither dissolve nor deteriorate in the presence of hexane vapor. To ensure optimum ultrasonic transmission across the Teflon bonding layers, a compressive stress was applied to the delay-rod–sample–delay-rod sandwich with three spring clamps, which also allowed the parallelism of the transducers to be accurately aligned.

The sample–delay-rod assembly was inserted into a transparent glass cell that had vacuum-tight seals between the glass cell and the cylindrical sides of the quartz delay rods. This allowed hexane vapor to be admitted to the sample while the transducers remained untouched by the vapor outside the cell, thus preventing the hexane from coming into contact with the epoxy bonds between the transducers and the delay rods. The cell was connected via a third port to a large ballast tank (3800.37 cm^3), a hexane reservoir, and a pumping system. Two Baratron gauges (dead volume 2.66 cm^3 each) were used to measure the pressure inside the ballast tank and the sample cell (dead volume 14.19 cm^3). The hexane reservoir was immersed in a temperature-controlled bath to control the vapor pressure in the sample cell. The gas handling system also allowed volumetric isotherm measurements to be made concurrently with the ultrasonic measurements.

This was accomplished by isolating the hexane reservoir from the cell and admitting (or extracting) hexane vapor to (or from) the ballast volume in precisely determined amounts as measured by the Baratron gauges. The temperature of the sample was 22.6 °C and was stabilized to better than 0.01 °C by immersing the cell in a second temperature-controlled bath.

Because of considerable attenuation in the Vycor sample and in the Teflon bonding layers, the ultrasonic measurements were performed in transmission rather than reflection by generating a short 3 μs pulse in one transducer and detecting the arrival time and amplitude of the transmitted pulse in the second transducer. The measurements were performed at four frequencies between 3 and 15 MHz by exciting the transducers either at their 2 MHz fundamental frequency or at one of their three lowest odd harmonics. Longitudinal waves were used exclusively in the present experiments. The sound velocity in the sample, 3.53 km/s, was determined from the transit time through the sample by using a simple pulse-echo overlap technique in which corrections for phase shifts at the sample delay-rod interfaces were taken into account. Changes in the velocity and attenuation were measured with a quadratic phase detector, which enabled changes in phase to be determined to better than 1 part in 10^6 and changes in amplitude to better than 0.02 dB.

As the ambient hexane vapor pressure was varied, the time evolution of the velocity and attenuation in the sample were monitored continuously in response to a small change in the pressure. However, transient inhomogeneities in the fluid distribution inside the pores of the Vycor limited the accuracy with which these dynamic measurements of changes in attenuation could be performed. As the pressure is varied, the hexane enters or leaves the sample rod radially, starting from the outer surface. Thus, while a new equilibrium configuration of fluid in the pores is being established, there is a radial concentration gradient of fluid in the sample, leading also to a radial gradient in the ultrasonic velocity and wavelength. Since the transducers have a larger diameter than the sample, the entire sample is irradiated with sound, but sound paths near the outside of the sample will have different wavelengths than those near the center; thus the relative phases of the waves arriving at different positions across the detecting transducer will no longer be the same as when the fluid distribution is uniform. This causes interference effects at the detecting transducer, leading generally to a decrease in the detected signal; this occurs because the measured voltage from the transducer is proportional to the spatial average of the ultrasonic field across its surface, and the variation in phase causes partial cancellation of this signal.

B. Light scattering measurements

The light scattering measurements were performed on a different piece of Vycor, which was shaped as a disk, about 2.5 cm in diameter and 6 mm thick. The disk was mounted in a sealed container connected to a reservoir tank of liquid hexane that was immersed in a temperature-controlled bath, allowing the pressure of the hexane vapor in the system to be set by varying the temperature of the bath. The sample cell had two flat windows, which allowed visual observation of the Vycor as the pressure was changed and also allowed a laser beam to be directed through the sample to measure both the transmission through the sample and the scattered light intensity. The 5145-Å line from an Ar^+ laser was used for these measurements.

The transmission of light through the sample was measured by placing a detector in the transmitted beam and measuring the intensity. Apertures were used to prevent scattered light from impinging on the detector, ensuring that only the unscattered transmitted intensity was measured. Because of the large number of interfaces in the beam, both those of the sample and those of the two windows, the transmission was reduced to 0.8, even when there was no scattering of the light within the Vycor.

The scattered light intensity was measured by placing a lens of a relatively large focal length in the beam immediately before the sample cell. This lens focused the laser beam through a small hole in a semitransparent scattering screen placed on the other side of the sample, in the focal plane of the lens. A beam absorber, made by drawing out a small piece of glass pipette and painting it black, effectively absorbed all the light transmitted through the hole in the screen. Because the screen was placed at the focal plane of the lens, it represents a Fourier transform plane with respect to both the lens and the sample, so that the scattering at the screen is equivalent to that in the far field. This scattered light intensity was measured by imaging the screen onto a charge-coupled-device (CCD) TV camera placed behind the screen. The image was digitized by a computer, averaged to improve the signal to noise ratio, and corrected for the background and the response of the screen and scattering system. The results were radially averaged to obtain $I(q)$, the dependence of the scattered intensity on wave vector, $q = 4\pi n \sin(\theta/2)/\lambda$, where n is the index of refraction of the Vycor, λ is the wavelength of the light in vacuum, and θ is the scattering angle.

The CCD camera was operated in the linear response mode, and the digitizer recorded 1 byte/pixel. Thus, the effective dynamic range for each image was limited to about two decades in intensity. To increase this dynamic range, several images were recorded with the incident laser adjusted to different power levels. At the low power levels, there was no saturation of the camera, but the intensities in the pixels at higher values of q were below the noise level and could not be measured reliably. By contrast, at the higher incident power levels, the intensities of the pixels at lower values of q were sufficient to saturate the digitizer and could not be measured. The unreliable pixels of each image were discarded, and the data sets were scaled by the relative incident power, allowing the calculated $I(q)$ to be combined to extend effectively the accessible dynamic range in intensity to over four decades. Similarly, the dynamic range in scattering angle was increased by recorded data separately, using lenses with two different focal lengths. The first had a focal length of 35 cm, providing better resolution of the high-q data, while the second had a focal length of 192 cm, pro-

viding better resolution, of the low-q data. The curves for $I(q)$ were again combined by scaling them so that the data matched in the overlapping regions of q. This effectively extended the dynamic range in q to about two and a half decades.

Over a small range in pressure of the ambient vapor, the Vycor scattered light very strongly, causing it to turn white in appearance. At this point, the scattering was so intense that the light was multiply scattered, precluding determination of its angular dependence. Thus scattering data were collected only when the transmitted light was reduced by no more than 10–15 %, limiting the range of pressures over which reliable data could be obtained.

III. SORPTION ISOTHERMS

The adsorption and desorption of fluid in a porous material such as Vycor are often characterized by means of a sorption isotherm, which is a measure of the mass uptake in the solid as the pressure of the ambient vapor is varied. This can be measured gravimetrically; the weight of the Vycor sample is measured as a function of the pressure of the ambient vapor. The sorption isotherm can also be measured volumetrically; a ballast tank of known volume is evacuated and then connected to the sample container. The pressure of the vapor in the ballast tank is measured both before and after it equilibrates with the sample, enabling both the change in volume of adsorbed gas and the ambient pressure to be determined.

An example of a gravimetrically determined sorption isotherm of hexane in Vycor is shown in Fig. 1, where we plot the change in mass of the sample relative to the mass of the empty sample, $\Delta M/M_0$, as a function of the pressure of the ambient vapor relative to the saturation pressure, P/P_s. The data obtained on adsorption are plotted as open points, while the data obtained on desorption are plotted as solid points. This isotherm was obtained by using the piece of Vycor used in the light scattering measurements. The sorption isotherm exhibits a pronounced hysteresis [12], which is characteristic of this class of porous material. The data obtained on adsorption rise monotonically from the lowest pressures until the maximum fluid uptake is achieved at a reduced pressure, $p=P/P_s$, of about 0.6. By contrast, the data obtained on desorption remain nearly constant as p is reduced from 1 all the way to about 0.4, whereupon they exhibit a precipitous drop, with more than half the fluid being desorbed over a span of about 0.02 in reduced pressure. As the pressure of the ambient vapor is decreased still further, the data for adsorption and desorption overlap.

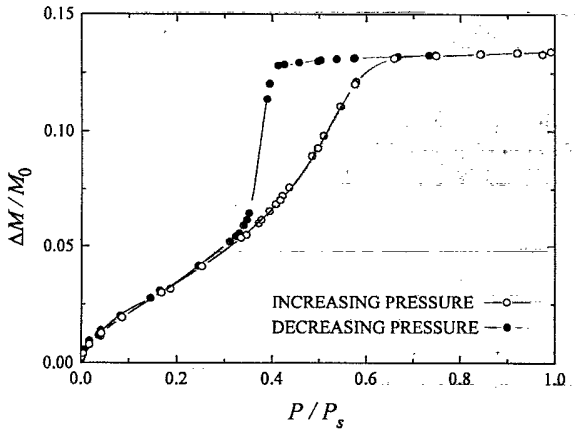

FIG. 1. Gravimetric sorption isotherm for hexane in the Vycor sample used in the light scattering experiments.

The origin of the hysteresis in the isotherm can be understood by considering the behavior of a single, straight pore of radius r. If the fluid is wetting, as in the case for hexane in Vycor, the ends of the pores become curved as p is reduced. The smallest radius of curvature is that of the pore itself, r, so that the average curvature is $2/r$, the sum of the two principal radii of curvature of the end cap. Because of the surface tension, the pressure on the vapor side is greater than that in the fluid, with the pressure difference given by the Laplace equation,

$$\Delta P=\frac{2\sigma}{r}\ , \tag{1}$$

where σ is the surface tension of the fluid. As p is decreased still further, the pore is drained; the decrease in condensation energy of the fluid due to this pressure difference across the curved interface results in a lowering of the saturation pressure, as given by the Kelvin equation [2],

$$\frac{P}{P_s}=e^{-\sigma V_m/rk_BT}\ , \tag{2}$$

where V_m is the molar volume of the fluid, k_B is Boltzmann's constant, and T is the temperature. The behavior on adsorption is markedly different. As the pressure of the ambient vapor is increased from zero, uptake of the fluid by the Vycor initially occurs through adsorption of the hexane molecules onto the interfaces of the pores of the Vycor. Thus, the average curvature of the interface is only $1/r$, necessitating a higher pressure of the ambient vapor to cause capillary condensation than was needed to start the pore drainage.

This difference in the radii of curvature on filling and emptying, due to the different geometries of the liquid-vapor interface, is the origin of the hysteresis in the sorption isotherm. Any real porous material will have a distribution of pore sizes and shapes, resulting in a more gradual increase in the rise of the sorption isotherm. Nevertheless, this method is extremely sensitive to the shape and distribution of pores; thus the sorption isotherms of different pieces of Vycor can be noticeably different, reflecting slight differences in the pores. For this reason, we measure the separate sorption isotherms for each piece of Vycor used in these experiments.

This sensitivity is also the basis for measurements of the distribution in pore sizes [1]. Because of the uncertainty in the shape of the interface as the fluid is adsorbed onto the solid, these measurements are normally done on desorption. The Kelvin equation is used to relate the pressure of the ambient vapor to the pore size, while the

amount of fluid desorbed determines the distribution of pores of each radius. Of course, this interpretation implicitly assumes that each pore is connected to the surface, so that at each pressure all pores of the radius determined by the Kelvin equation can be drained. Thus, verifying this assumption of connectivity is essential in confirming the reliability of this method of determining the pore size distribution.

IV. FLUID ADSORPTION

In this section, we show how ultrasonic velocity and attenuation measurements can be used to obtain information on the behavior of the fluid in the pores during adsorption, concentrating especially on the final stages of filling. These experiments probe the geometrical configurations of the liquid and vapor on filling and test the predictions of some current models for the adsorption process. In addition to providing information on the fluid mass uptake, these ultrasonic data also allow us to infer the presence of uncorrelated vapor voids that form over the range of ambient pressures over which at least some of the individual pores become completely filled by capillary condensation. This behavior contrasts strongly with our observations during desorption and is an important manifestation of the dramatic differences that are found on filling and drainage.

The velocity of longitudinal ultrasonic waves in Vycor is determined by its longitudinal elastic modulus β and density ρ via the relation

$$v=\sqrt{\beta/\rho}\ . \tag{3}$$

Thus, as fluid is added to the pore space by increasing the ambient vapor pressure, the change in the sound velocity reflects a competition between the increase in modulus (which tends to increase the velocity) and the increase in total density due to the mass of the adsorbed fluid (which tends to decrease the velocity). Rewriting Eq. (3) in terms of changes in the ultrasonic transit time $t=L/v$ and solving for the relative change in the sample mass due to the adsorbed fluid gives

$$\frac{\Delta M}{M_0}=\frac{\Delta\rho}{\rho_0}=2\frac{\Delta t}{t_0}+\left[\frac{\Delta t}{t_0}\right]^2+\frac{\Delta\beta}{\beta_0}\left[1+2\frac{\Delta t}{t_0}+\left[\frac{\Delta t}{t_0}\right]^2\right]$$
$$\approx 2\frac{\Delta t}{t_0}+\frac{\Delta\beta}{\beta_0}\ , \tag{4}$$

where the subscript 0 denotes values in empty Vycor, and the second approximate relation holds for small changes in the transit time and modulus. When the longitudinal modulus is unaffected by the adsorbed fluid, as would be expected at least for low adsorbate concentrations, the change in the relative mass is equal to twice the change in the relative transit time. Then the relative transit time provides an accurate and sensitive measure of the adsorption isotherm [13]. Conversely, if the relative mass change is determined independently by a separate measurement of the adsorption isotherm, Eq. (4) can be used to obtain the variation of the modulus.

Figure 2(a) shows a comparison of $\Delta t/t_0$ with

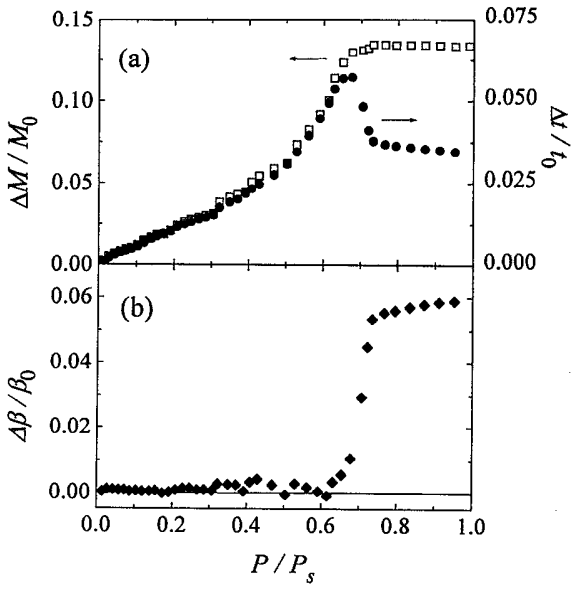

FIG. 2. (a) Comparison of the relative change in the mass, $\Delta M/M_0$, and ultrasonic transit time, $\Delta t/t_0$, on adsorption. Note the difference of a factor of 2 in the vertical scales. (b) Relative change in the longitudinal modulus, $\Delta\beta/\beta_0$, calculated from the data shown in (a).

$\Delta M/M_0$, which was measured simultaneously from the volumetric isotherm. The ultrasonic data were taken at a frequency of 6.2 MHz, which corresponds to a wavelength of 570 μm. Note that the y-axis scale for the isotherm data is twice that of the transit time data. This figure clearly shows the remarkable fact that, for pressures all the way up to $p\approx 0.7$, the increase in the relative transit time is almost exactly equal to half the increase in the relative mass; the slight discrepancy between these two quantities for $0.5<p<0.7$ is entirely accounted for by the quadratic terms in Eq. (4). Thus, the modulus is unaffected by adsorbed layers of fluid until the pores become *completely* filled. This is shown in Fig. 2(b), where we plot the relative change in the longitudinal modulus that is calculated directly from our ultrasonic transit time and volumetric isotherm data, using Eq. (4). There is no significant variation in the modulus until $p\approx 0.7$, although the fluctuations in the calculated modulus are greater than those in either the transit time or isotherm data because calculating the modulus from the data involves taking the difference of two nearly equal quantities. At $p\approx 0.7$, there is a very sudden increase in the modulus of about 5%, followed by a gentle rise to a final value, at $p=1$, that is nearly 6% larger than the modulus of empty Vycor.

Before discussing in greater detail the novel features of these data, we first use a conventional analysis of our isotherm measurements to determine the surface area and porosity of our Vycor sample. The surface area of porous materials is frequently determined from measurements of the fluid mass uptake at low pressures by using the adsorption model of Brunauer, Emmett, and Teller (BET) [14]. Applying this model to our combined ultrasonic

and volumetric isotherm data shows that complete monolayer coverage occurs at $\Delta M/M_0=0.036$, corresponding to 27% of the total fluid mass uptake. Using an estimated value for the cross-sectional area of a hexane molecule of 40 Å^2, we find that the surface area for our sample is ≈ 100 m^2/g, in good agreement with other measurements [7,13]. We note that this assumes that the anisotropic hexane molecule is preferentially oriented with its long axis parallel to the surface; any model that assumes that the long axis is oriented perpendicular to the surface gives an area that is not consistent with our isotherm data. The net change in mass of the Vycor when the pores are completely filled with hexane (density $\rho=0.6603$ g/cm^3 [15]) is 13.4%, allowing us to determine the porosity, $\phi\approx 0.309$. This number agrees well with a value of the porosity, $\phi=0.304$, calculated from the measured density of the dry Vycor sample ($\rho=1.54$ g/cm^3), assuming that the density of solid glass matrix is the same as fused quartz ($\rho=2.20$ g/cm^3 [16]).

The changes in the Vycor modulus observed in Fig. 2 directly reflect the dramatic changes that occur in the effective hexane modulus. This can be shown from the effective medium model for sound propagation in a fluid-filled porous solid that was developed by Biot [17,18]. There are two important frequency regimes in Biot's theory, depending on the ratio of the mean pore radius r to the viscous penetration depth $\delta=(2\mu/\rho_H\omega)^{1/2}$. Here μ and ρ_H are the fluid viscosity and density and $\omega/2\pi$ is the ultrasonic frequency. At high frequencies, $\delta \ll r$, the fluid and solid are only weakly coupled together, with the result that a second, slow, longitudinal mode is predicted. However, for our range of ultrasonic frequencies, $\delta \cong 2000$ Å $\gg r$, so that the fluid is viscously locked to the Vycor matrix and only a single longitudinal mode can propagate. In this limit, Biot's theory predicts that the change in the Vycor modulus due to the fluid is given by

$$\frac{\Delta\beta}{\beta_0}=\frac{(K_Q-K_0)^2\beta_H/\beta_0}{\phi K_Q^2+[(1-\phi)K_Q-K_0]\beta_H}\approx\frac{1}{\phi}\left[1-\frac{K_0}{K_Q}\right]^2\frac{\beta_H}{\beta_0}, \tag{5}$$

where ϕ is the porosity, K_Q is the bulk modulus of the amorphous quartz glass that makes up the Vycor matrix, and K_0 is the bulk modulus of empty Vycor. The second, approximate expression is valid when the modulus of the fluid is much less than that of the solid; for hexane in Vycor, the error involved in this approximation is no more than a few percent. Thus, to a good approximation, the change in the Vycor modulus is proportional to the effective fluid modulus β_H, enabling the latter to be investigated under the very unusual conditions to which the fluid is subject in porous media.

Biot's theory also gives a prediction, in terms of β_0, K_0, β_H, K_Q, and ϕ, for the total change in the Vycor modulus when the pores are filled at the saturated vapor pressure. Using our measured values of the longitudinal and shear wave velocities for the empty Vycor sample, $v_l=3.53$ km/s and $v_s=2.11$ km/s, we determine that $\beta_0=\rho v_l^2=1.92\times10^{10}$ Pa and $K_0=\beta_0-\frac{4}{3}G_0=1.01\times10^{10}$ Pa, where $G_0=\rho v_s^2=6.86\times10^9$ Pa is the shear modulus. Combining these results with literature values of the quartz modulus, $K_Q=3.03\times10^{10}$ Pa [16], and the liquid hexane modulus, $\beta_L=8.03\times10^8$ Pa [19,20], we find that Eq. (5) predicts that $\Delta\beta/\beta_0=0.0584$, which is in exceptionally good agreement with our experimental value of 0.059. This excellent agreement at $p=1$, where the hexane modulus is known from other measurements, demonstrates that Biot's theory can be used quantitatively to investigate the behavior of the hexane modulus in the Vycor matrix at low pressures, where other effects cause it to be reduced.

A second effective medium theory can be used to gain insight into the remarkable observation that the modulus of Vycor is unaffected by the adsorption of vapor until the pores are virtually all filled with liquid. The origin of this behavior is the presence of vapor voids, which persist in the pores right up to the final stages of filling. At low pressures, a liquid layer builds up on the pore walls and the voids form a continuous network connected to the vapor reservoir outside the sample. Above $p\approx0.45$, the necks and small pores begin to fill by capillary condensation, thus forming vapor bubbles, which shrink in size as the ambient vapor pressure is increased further. The bubbles do not disappear, however, until the pore space is completely filled with liquid. For bulk liquids, the presence of these vapor voids has a dramatic effect on the modulus of the fluid, as can be seen from Wood's approximation [21] for the effective modulus of a liquid-vapor mixture:

$$\frac{1}{\beta_H}=\frac{1-\phi_V}{\beta_L}+\frac{\phi_V}{\beta_V}, \tag{6}$$

where β_H, β_L, and β_V are the moduli of the hexane fluid mixture, the liquid, and the vapor, respectively, and ϕ_V is the volume fraction of vapor in the pores. In this approximation, the compressibilities ($1/\beta$) of the liquid and vapor are added in proportion to their volume fractions, so that the effective modulus of the fluid mixture is dominated by the very weak modulus of the vapor voids. Thus this simple effective medium approximation predicts that the modulus of the fluid-vapor mixture is so small for $\phi_V \geq 10^{-3}$ that it makes a negligible contribution to the total Vycor modulus. The sharp rise in $\Delta\beta/\beta_0$ at $p\approx0.7$ is therefore a *direct* measure of the dramatic increase in the hexane-bubble modulus as the vapor bubbles in the remaining 1% of the pore space are filled.

Additional information on the presence of vapor microbubbles during filling by capillary condensation is provided by the ultrasonic attenuation. As shown by the open circles in Fig. 3, the excess attenuation relative to empty Vycor exhibits a large, asymmetric peak that is centered near $p\approx0.7$, where the sudden increase in the modulus is observed. At higher pressures there is a sharp cutoff in the attenuation as all of the pores become completely filled; at lower pressures the attenuation decreases more gradually, extending down to $p\approx0.45$, where capillary condensation first occurs in the smallest pores. Thus the attenuation is a maximum when the bubbles occupy about 1% of the pore space, and attenuation is observed over the entire range of pressures for which vapor bub-

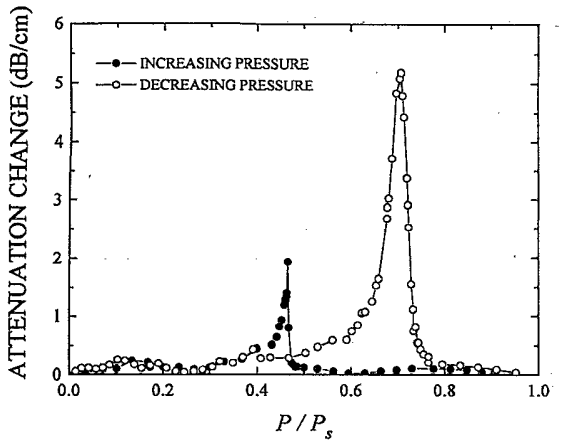

FIG. 3. Change in the ultrasonic attenuation during filling (open symbols) and drainage (closed symbols) at a frequency of 6.2 MHz.

bles are present. This strongly suggests that the attenuation is caused by the vapor bubbles. From the Laplace and Kelvin equations, Eqs. (1) and (2), we estimate that the average radius of these vapor bubbles is $r \approx 50$ Å at the attenuation peak; this is somewhat larger than the radius of pores and is consistent with the last vapor bubbles remaining the larger pore spaces; for example, where several pores meet. The frequency dependence of the attenuation indicates that the dominant interaction mechanism is absorption and not scattering; the attenuation varies approximately as $\omega^{1.4}$ for frequencies between 3 and 15 MHz. Although these data do not extend over a very large range of frequencies, they are clearly sufficient to rule out any scattering mechanism since in this case the attenuation would vary as ω^4, as the ultrasonic wavelengths are much larger than the size of possible scattering sites in Vycor. By contrast, absorption mechanisms usually have a quadratic or lower frequency dependence, the exact power law depending generally on the proximity of the inverse frequency to the relevant time scales in the system. Thus only an ultrasonic absorption mechanism is consistent with our data.

We believe that this large attenuation is caused by an additional form of motion of the fluid that is possible when the pores are partially filled with liquid [22]. We assume that, in response to the pressure fluctuations created by the sound, the pore space in the Vycor "breathes" so as to sinusoidally squeeze the liquid and vapor contained in the pores. There are two possible responses of the liquid to this "breathing" of the pore space; it can be compressed, thereby accommodating all the change in volume of the pore space; or it can flow axially along the pores, thereby compressing the vapor to accommodate the change in volume. When the pores are completely filled with liquid, the liquid must be compressed and no significant axial flow can occur. By contrast, for partially saturated porous media, the vapor is significantly more compressible, and thus one might expect that all of the volume change is taken up by the vapor, resulting in appreciable viscous flow of the liquid along the pores. This is, in fact, true for low frequencies and leads to a much larger dissipation (and concomitant large attenuation of the sound) then would be observed at the same frequency if only compression of the liquid were possible. Furthermore, at higher frequencies, the viscous resistance in the liquid can become large enough that it is easier to compress the liquid than to make it flow along the pores. The crossover between these two flow regimes yields a complicated frequency dependence of the attenuation. This can account for the frequency dependence observed in our experiments.

V. FLUID DESORPTION

The behavior on draining the hexane from the Vycor is markedly different than that observed during filling. We summarize this behavior in Fig. 4, where we compare the volumetric desorption isotherm with the change in the relative transit time and the calculated change in modulus. All three sets of data exhibit pronounced drops over a very narrow range in pressures, around a reduced pressure of $p \approx 0.5$. This pressure is significantly less than the pressure at which the pores are filled because of the capillary condensation on adsorption, reflecting the hysteresis in the isotherm. Moreover, the pronounced maximum in the transit time observed on filling [cf. Fig. 2(a)] is absent on draining. These dramatic differences reflect the different physics on desorption as compared to adsorption.

As the ambient vapor pressure is first reduced from the saturation value to about 0.5 of P_s, the desorption isotherm shows that the mass of sample decreases only a small amount. By comparison, as shown in Fig. 4(a), over the same range in ambient pressure, the transit time

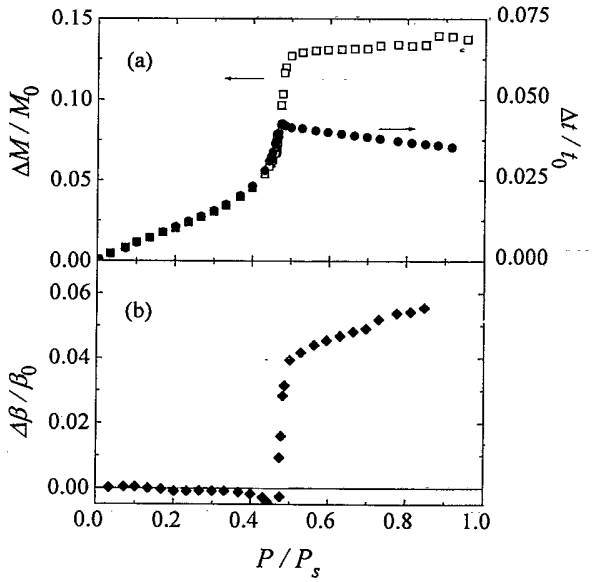

FIG. 4. (a) Relative change in the mass, $\Delta M/M_0$, and ultrasonic transit time, $\Delta t/t_0$, on desorption. (b) Relative change in the longitudinal modulus, $\Delta\beta/\beta_0$, calculated from the data shown in (a).

increases by a small but noticeable amount. For P greater than about 0.75, the change in transit time measured on draining exactly matches that measured on filling. However, the sharp rise at slightly lower pressures evident in the adsorption data is completely absent from the desorption data. Moreover, as shown by the solid symbols in Fig. 3, the large increase in the sound attenuation caused by the vapor microbubbles at $p \approx 0.7$ is also completely absent from the attenuation data. Thus, we conclude that no vapor bubbles are formed in the hexane within the pore space on draining for pressures all the way down to $p \approx 0.48$. Instead, the decrease in the mass must reflect the lowering of the hexane density due to very large negative pressures in the fluid within the pores and a concomitant drainage of hexane that still leaves the pores completely filled. These negative fluid pressures are caused by the curvature of the interface as the ambient vapor pressure is reduced. They can be calculated with the Laplace and Kelvin equations, and are as low as -130 atm.

Over this range of pressures, from $p \approx 1$ to $p \approx 0.5$, the decrease in the mass of the sample should, by itself, cause the relative transit time to decrease with p. Instead, however, the relative transit time increases by about 0.007. Thus, to account for both the decrease in mass and the increase in transit time, the modulus must exhibit a significant decrease, by ~ 0.02, as shown in Fig. 4(b). This decrease in modulus can only result from the very large negative pressures in the fluid within the pores, which can affect the modulus of both the hexane and the solid Vycor. We can estimate the change in modulus of the hexane by extrapolating pressure-dependent measurements of the velocity to negative pressures. This can account for roughly half of the total decrease in modulus. The larger decrease in the modulus observed here may result from a further softening of the modulus of the hexane as it approaches the spinodal line where β goes to zero. Although this stability limit has not been directly observed for hexane because of the extreme technical difficulties of achieving the required large negative pressures, we estimate that it is likely to be reached in the range of pressures between -200 and -500 atm based on investigations of other liquids [23,24]. Thus it is quite conceivable that this effect is important at the largest negative pressures reached in Vycor. In addition, the large negative pressure may also reduce the modulus of the Vycor matrix.

The very sharp decrease in relative mass observed in the desorption isotherm occurs over a range of reduced pressures of less than 0.03, around $p \approx 0.47$. In the first part of this range as p decreases, the transit time does not vary at all, while the reduced mass decreases sharply, indicating that about 30% of the total hexane has been drained. At this point, the relative transit time becomes equal to $\Delta M/2M_0$ and begins to decrease with decreasing p, directly reflecting the decreasing mass as the remainder of the hexane is drained. Over this range the relative change in the transit time measured on desorption is identical to that measured on adsorption. The sharp drop in mass just above $p \approx 0.47$, along with the lack of change in the transit time, means that the modulus must decrease precipitously, reflecting a substantial softening of the medium. By analogy to the behavior observed on filling, this suggests that large voids are formed in the pore volume as soon as the hexane drainage begins. By the time $p \approx 0.47$ and 30% of the total hexane has drained, the modulus has been reduced to the value of the empty Vycor, as seen in Fig. 4(b). In fact, the figure indicates that the modulus actually decreases below that of the empty Vycor. This behavior is unphysical and must reflect large inhomogeneities in the Vycor as the drainage proceeds from the outer surface in toward the central core of the sample. Because of phase cancellation at the detector, these inhomogeneities can produce somewhat larger changes in the measured transit time than actually occur.

Further evidence for these large-scale inhomogeneities is seen in the ultrasonic attenuation data. As shown in Fig. 3, the attenuation exhibits a very sharp peak when the relative mass of the sample begins to change because of the draining of the hexane. This peak in the attenuation is not as large in magnitude as that observed during the filling of the Vycor; however, it is considerably more narrow. That this peak is caused by large-scale inhomogeneities is evident from the highly unusual frequency dependence. We illustrate this in Fig. 5, where we plot the attenuation measured at several pressures as a function of frequency. No trend whatsoever is observed; instead, the data are completely random, increasing or decreasing, or even going through a peak, with frequency. Thus, the value of p at which the peak occurs depends somewhat on the frequency used to measure the attenuation; however, a peak is observed for each frequency at a pressure within the narrow range of p over which rapid drainage occurs. The origin of this attenuation is again the large spatial inhomogeneities in the Vycor as the hexane is drained and voids are formed, leading to interference effects at the detector, which manifest themselves as an increase in the observed attenuation, with large and erratic frequency variations rather than the usual behavior expected for absorption or scattering.

To characterize these inhomogeneities better, we mea-

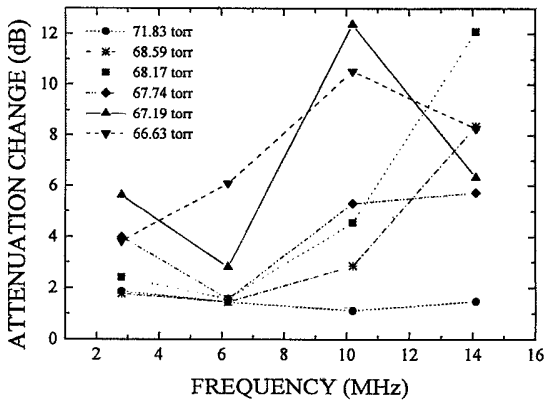

FIG. 5. Frequency dependence of the ultrasonic attenuation near the sharp peak on desorption.

sure the amount of light scattering by the Vycor. On filling, the transmission is essentially constant, although a small dip is observed when capillary condensation first begins to occur. The behavior of the transmission on draining is dramatically different. Over the range in pressures at which the hexane drains, the transmission exhibits a very sharp and narrow dip, as shown in Fig. 6. The beginning of the dip corresponds to the pressures at which the hexane just begins to drain, while the minimum transmission occurs at pressures at which a large fraction, but not all, of the hexane has drained. When the pressure is first decreased, the transmission varies somewhat across the sample; however, eventually the transmission becomes uniform across the sample as it is held at the new pressure. The time to achieve uniform transmission can be many hours. All the data shown in Fig. 6 were collected after the sample had equilibrated and the transmission was spatially uniform.

The origin of this sharp dip in the transmission is very strong scattering of light within the Vycor. This causes the Vycor to turn white and allows the scattering regions, and the spatial inhomogeneities, to be directly observed visually. When p is adjusted to the value where the relative mass just begins to decrease, the white regions appear initially as spots on the surface of the Vycor. This is illustrated in Fig. 7, which is a picture of the Vycor sample viewed through the windows of the cell and recorded by imaging the surface of the sample onto the CCD camera and digitizing the image. The sample is illuminated from behind, and thus the white spots on the surface scattering light and appear as darker regions. Some regions toward the center appear even darker because of white regions at both interfaces. If the sample is maintained at a constant pressure, the scattering regions expand to cover uniformly the surface of the sample. However, large inhomogeneities do persist, as the scattering regions are clearly confined to the surface and do not extend all the way into the Vycor. It is only when the pressure is further lowered by a small amount that the white regions appear to extend all the way into the sample. Thus, the Vycor clearly drains in from the surface. Similar behavior will occur for the rod-shaped sample used for the ultrasonic measurements. Initially, only the outer ring will drain, while the center will remain saturated. The resultant inhomogeneity will lead to the observed attenuation and will cause the dip in the calculated modulus.

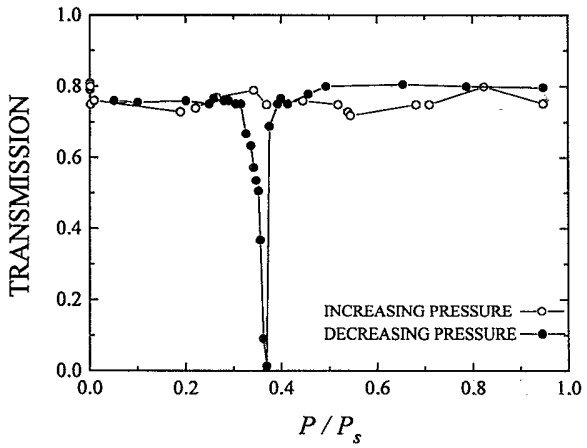

FIG. 6. Transmission of light through Vycor on adsorption (open symbols) and desorption (closed symbols).

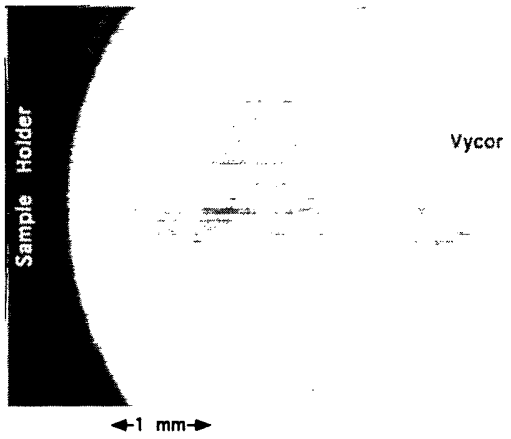

FIG. 7. Picture of Vycor as p is lowered to a value near the edge of the sharp drop in the desorption isotherm where the sample begins to turn white. The sample is illuminated from behind so that the white spots that scatter light appear dark.

This intense scattering of the light must be caused by the draining pores. When the Vycor is empty, there is a relatively large mismatch in the index of refraction between the empty pores and the surrounding glass; however, the size of each pore is very small, and, over length scales comparable to the wavelength of light, their density appears homogeneous. Thus, there is relatively little scattering of light. When the pores are completely saturated with fluid, there is virtually no mismatch in the index of refraction, and the scattering is reduced even further. However, when the Vycor drains, only some of the pores are emptied. All the surrounding pores are still filled with fluid and are thus index matched to the glass so that they do not contribute any scattering. By contrast, the empty pores can form structures with much larger range correlations; the size of these can be larger than the wavelength of light. This will result in very strong light scattering, much stronger than that of either the empty or the filled Vycor.

We determine the structure of these correlated regions by measuring the angular dependence of the scattered light. This can only be done at values of p between about 0.39 and 0.40 for this sample. At higher pressures, the scattering is too weak to exhibit any significant angular dependence, while at lower pressures, the scattering is so intense that multiple scattering significantly distorts the observed behavior.

We show the angular dependence of the scattered light when $p \approx 0.39$ in a logarithmic plot in Fig. 8. The exhibit a power-law behavior over an extended range. Thus the structure of the correlated regions of drained pores must be fractal. The slope of the data in Fig. 8 provides a mea-

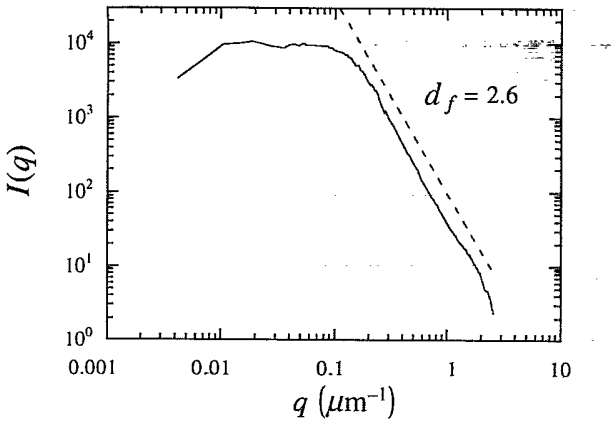

FIG. 8. Variation of the scattered light intensity with wave vector, showing the fractal correlations of the empty pores. The fractal dimension is $d_f=2.6$, as indicated by the slope of the solid line.

sure of the fractal dimension, $d_f \approx 2.6$, as illustrated by the solid line beside the data. At values of q around 0.1 μm^{-1}, the data saturate and become independent of q for smaller values. If the pressure is reduced slightly, the scattering at large q remains identical to that shown in Fig. 8, while the crossover shifts to somewhat smaller values of q. We emphasize that it is only the drained pores, which are surrounded by filled pores, that exhibit these fractal correlations; when the pore space is completely empty, the pores themselves do not have fractal correlations, as indicated by the isotropic scattering from the dry Vycor.

The correlations must result from the restricted connectivity of the pore space to the surface of the Vycor. Even though a larger number of pores can be drained at a given value of p according to the Kelvin equation, not all of these are actually drained because the access to the surface of many of these pores is blocked by smaller pores that still cannot drain. It is only those pores that are connected to the surface through even larger pores that drain as the appropriate value of p is reached. This results in the fractal correlations of the empty pores.

Further insight into this behavior can be obtained by the recognition that, at least initially, the drainage process is analogous to invasion percolation [9]. Invasion percolation occurs when a nonwetting fluid is forced into a porous medium containing a wetting fluid and when the rate of injection is so slow that all motion is dominated by capillary effects. Then, the invading fluid can only be injected into a pore if the applied pressure is larger than the Laplace pressure across the interface at the pore. However, a pore will only be filled with the injected fluid if it is connected to the source of this fluid, and this can only occur if all the pores connecting it to the source have larger diameters. This process can be mapped onto bond percolation and leads to a fractal structure for the flooded pores. In three dimensions, the fractal dimension is predicted to $d_f \approx 2.5$.

In the case of the draining of the Vycor, the hexane wets the surface of the Vycor, while the vapor represents the nonwetting fluid. At the early stages of the drainage, the process is identical to invasion percolation, accounting for the fractal correlations of the emptied pores. The measured value of the fractal dimension is in excellent accord with that expected for invasion percolation. As the drainage proceeds, the range of the fractal structures grows, and their correlation length becomes larger. Barring any large-scale inhomogeneities in the sample, the correlation length should ultimately extend to the full thickness of the Vycor. As further drainage proceeds, the pores between the fractal structures are drained, causing the correlation length to begin to decrease. At this point, the direct analogy to invasion percolation breaks down; ultimately all pores are drained, whereas, by contrast, not all pores are filled with an injecting fluid.

Fractal correlations in draining Vycor have been reported previously [25,26]. The value of the fractal dimension obtained in the neutron scattering experiments was $d_f \approx 1.75$, substantially less than that obtained in our experiments. However, these observations were based on small angle neutron scattering results, which probed structures at much larger values of q and limited the observations to the early onset of the fractal correlations. Thus, it is possible that the neutron scattering results were still susceptible to effects due to short-range correlations in the pore structure, masking the true fractal correlations in the drained pores.

Our results clearly show that connectivity plays a critical role in the drainage process of a fluid from a porous medium. Thus any determination of the distribution of pore sizes using the sorption isotherm and the Kelvin equation that ignores the consequences of this connectivity will be invalid. This calls into question many commonly used methods. The importance of the connectivity in the measurements of pore size distributions in porous materials has been considered previously, but there is, as yet, no satisfactory method to incorporate these effects properly. This remains a key challenge in the study of porous materials.

VI. TIME-DEPENDENT BEHAVIOR

To learn more about the physics of adsorption and desorption, we also measured the time for fluid to diffuse into or out of the pores in response to a step change in the external vapor pressure. This was investigated during the ultrasonic and concurrent volumetric isotherm experiments by recording the time dependence of the changes in adsorbed fluid mass, ultrasonic transit time, and attenuation as the external pressure was varied. Because the pore space of Vycor is so narrow and tortuous, the characteristic time for fluid to enter or leave the sample is generally extremely long. Remarkably, it also varies by several orders of magnitude during filling and drainage as the dominant mechanism for mass transport changes. Of particular interest is the desorption behavior in the critical regime, where substantial amounts of fluid first begin to leave the sample and fractal correlations in the empty pore space are observed; in this regime, the flow of fluid

from the pores does not reach an equilibrium configuration on a time scale of days and is extremely sensitive to very small fluctuations in the ambient conditions.

Apart from the behavior in the critical desorption region, the transport of fluid into or out of the pores is expected to be well described by using a diffusion model. For the cylindrical sample used in these experiments, the fluid diffuses radially, and the solution of the diffusion equation for the mass of fluid, $m(t)-m_0$, that has entered or left the sample after a step change in the pressure at time $t=0$ is given by [27]

$$m(t)=m_0+\delta m\left[1-\sum_{n=1}^{\infty}\frac{4}{a^2\alpha_n^2}\exp(-D\alpha_n^2 t)\right], \quad (7)$$

where m_0 is the mass of fluid present uniformly in the sample at $t=0$, δm is the total change in fluid mass after infinite time, a is the sample radius, $a\alpha_n$ are the roots of the zeroth order Bessel function of the first kind, D is the diffusion coefficient, and t is the time. Thus the diffusion coefficient D can be obtained by fitting this expression to time-dependent adsorption data; D can also be obtained from changes in ultrasonic transit time and attenuation with time, provided that the variation in these quantities is proportional to the change in the mass of adsorbed fluid.[1] At long times, $t \geq a^2/5D$, the behavior is dominated by the first term in the sum over n, and a single exponential decay is observed.

It should be noted that Eq. (7) is the solution of the diffusion equation, under the assumption that the final pressure after the step change remains constant. For volumetric isotherm measurements, this condition cannot be strictly met because of the finite size of the ballast reservoir. However, in our experiments, the large ballast volume used ensured that the variation in the ambient pressure following a step change in p was an extremely small fraction of the total pressure change, and this small variation resulted in an insignificant distortion of the observed time dependence. The only exception occurred during the sharp drop in $\Delta M/M_0$ on desorption, when the quantities of fluid leaving the Vycor sample were so large that, even using our very large ballast volume, the resulting pressure increase after the step was actually found to exceed the initial step change in p; in this regime, volumetric isotherm measurements of the time dependence were not feasible, and meaningful data could only be obtained with the sample connected to a liquid hexane reservoir maintained at constant temperature. Thus, in this regime, we were only able to investigate time-dependent behavior by using measurements of the ultrasonic transit time and attenuation.

A typical set of data, taken during desorption as the reduced pressure p was changed from 0.331 to 0.299, is shown in Fig. 9. These data are representative of the behavior observed at reduced pressures up to about 0.7 on adsorption and below about 0.45 on desorption. Figure 9(a) shows the variation with time of the relative mass $\Delta M/M_0$ of hexane in the Vycor sample, calculated from the variation in the pressure of the hexane vapor surrounding the sample during the volumetric isotherm

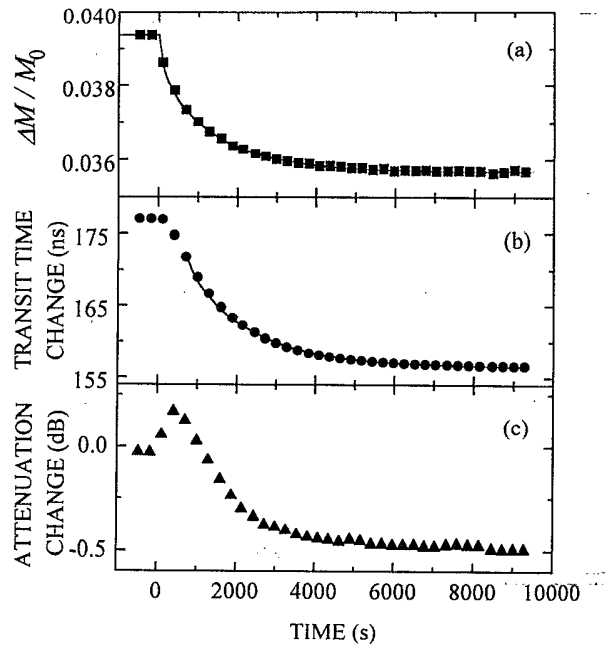

FIG. 9. Time dependence of (a) the relative mass, $\Delta M/M_0$; (b) the ultrasonic transit time; and (c) the ultrasonic attenuation as the relative pressure is lowered from 0.331 to 0.299 at time $t=0$ s. The solid lines show the results of fitting Eq. (7) to the data, as described in the text.

measurements. As is the case for all the time-dependent graphs presented in this section, the zero of the time axis coincides with the time at which the pressure was changed abruptly to its new value. The solid curve in Fig. 9(a) shows the best least-squares fit of Eq. (7) to these data, with D as an adjustable parameter but with δm fixed by the condition that the total variation in $m(t)$ be given by the difference between m_0 and the infinite time limit of $m(t)$ as determined directly from the data. In the fit, only the first eight terms is the sum were included since the terms for higher n fall to zero so quickly that their contribution even to the first data point for $t>0$ is negligible; these higher-order terms do, of course, make a small contribution ($\approx 5\%$) at $t=0$ to the second term in Eq. (7), and this was correctly taken into account by determining δm as outlined above. It can be seen from this figure that the diffusion model gives an excellent description of the measured time dependence of $\Delta M/M_0$, implying that accurate values of the diffusion coefficients can be determined from these data. For the data shown in this figure, we obtain $D=1.52\times10^{-5}$ cm^2/s.

Figures 9(b) and 9(c) show the variation in the ultrasonic transit time and attenuation measured at 6.2 MHz, due to the change in the mass of absorbed fluid shown in Fig. 9(a). Because of the diffraction and interference effects discussed in Sec. II, the time dependence of $\Delta t/t_0$ does not track the time dependence of $\Delta M/M_0$ exactly, allowing only approximate values of the diffusion coefficient to be obtained by fitting Eq. (7) to the transit time data. In particular, the measured transit

time underestimates the initial distribution of fluid in the sample just after the pressure has been changed, although it follows the later time behavior (when the fluid has penetrated further into the sample) quite closely. To account for this, the first couple of data points were excluded from the fit of Eq. (7) to the transit time data. The solid curve in Fig. 9(b) shows the result of this fit, giving a value for D of 1.3×10^{-5} cm^2/s, which is within 20% of the value found from the isotherm data. The change in the attenuation, shown in Fig. 9(c), further confirms that the discrepancies in the time dependence of $\Delta t/t_0$ arise from subtle phase interference effects resulting from the fluid nonuniformity. As can be seen from the figure, the attenuation initially undergoes a very small increase just after the pressure is lowered, followed at later times by a somewhat larger decrease as the final equilibrium value is reached. Thus, the attenuation is greatest when the fluid inhomogeneity is largest and is not a direct measure of the total change in fluid concentration. Therefore, a diffusion coefficient cannot be determined from these attenuation data.

The variation of the apparent diffusion coefficient with pressure on both filling and drainage is shown in Fig. 10. Except for the data at the highest pressures, which are discussed in more detail below, these diffusion coefficients were determined from the isotherm data for $\Delta M/M_0$. Data taken for increasing pressure are indicated by open circles and for decreasing pressure by closed circles, with the dashed and solid lines serving as guides to the eye. For reduced pressures up to about 0.6 on filling and below 0.4 on draining, the diffusion coefficient is relatively independent of pressure, having values varying from 6×10^{-6} to 2×10^{-5} cm^2/s, with D typically being on the order of 1×10^{-5} cm^2/s for most pressures in this range. We identify these values of D with surface diffusion, which is the dominant transport mechanism in the pressure range where the pore walls are covered with an adsorbed film, but where none of the pores are filled by capillary condensation. It is interesting that these values of the surface diffusion coefficient are comparable to measured values (ranging from 9.9×10^{-6} cm^2/s to 1.24×10^{-5} cm^2/s) of the self-diffusion coefficient of liquid hexane in Vycor [28]. Also, these values of the surface diffusion coefficient are approximately smaller by a factor of 5 than the surface diffusion coefficient of toluene in Vycor at the same temperature [29].

On adsorption, above a reduced pressure of about 0.45 (corresponding to the lowest pressure at which hysteresis is observed in the isotherm) we expect that surface diffusion is combined with capillary condensation flow, since some of the pores are likely to become completely filled above this pressure. However, no dramatic change in the diffusion coefficient is observed until $p>0.6$, whereupon the diffusion coefficient increases rapidly as the majority of the pores finally become filled. Once the pores are completely filled, the diffusion coefficient has increased by more than two orders of magnitude, reflecting a completely different mechanism for fluid transport in the pores. In this range of external pressures, above $p\approx0.7$ on adsorption and down to $p\approx0.5$ on desorption, the fluid mass changes only because of a change in the fluid pressure inside the pores. This occurs because the fluid pressure becomes less negative as the curvature of the meniscus of the surface pores is reduced at higher external pressures, thereby increasing the fluid density. Since the pore volume remains fixed, this also increases the mass of fluid in the pores. Thus the relevant time scale for fluid mass transport is now determined by the time for the fluid pressure in the pores to reach a new equilibrium value when the external pressure is varied. This time is very short (≈10 s) compared with the diffusion time found at lower pressures (≈1 h) as can be seen from the typical data for this pressure range shown in Fig. 11. These data on the time response were deter-

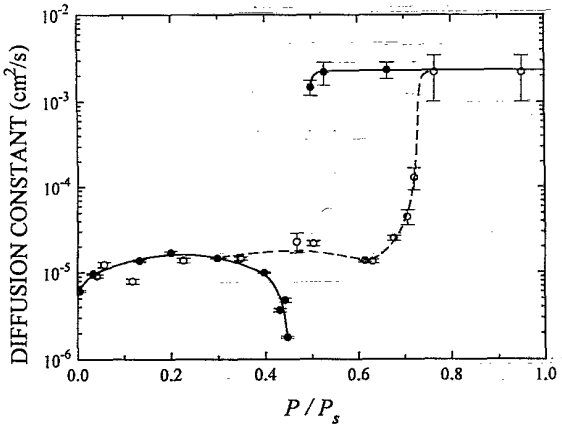

FIG. 10. Pressure dependence of the diffusion coefficient for fluid mass transfer in Vycor on adsorption (open symbols) and desorption (closed symbols). The lines are guides to the eye. *Note* the gap in the data for $0.48>p>0.45$ on desorption, where the diffusion model fails to describe the fluid drainage.

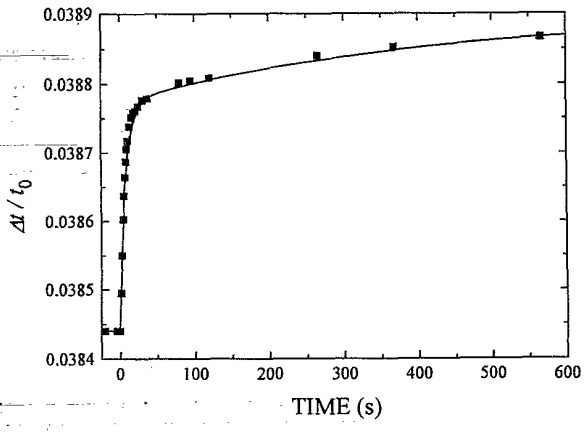

FIG. 11. Time dependence of the relative transit time change as p is lowered from 0.6968 to 0.6636 in the pressure range where the pores remain full. The solid line shows a theoretical fit in which the rapid response is described by diffusion, with a diffusion coefficient $D_P=2.3\times10^{-3}$ cm^2/s. In addition, there is a slower relaxational response with a time constant of 370 s.

mined from the ultrasonic velocity, rather than from the volumetric isotherm, because of the greater sensitivity of the velocity measurements to very small changes that occur in this pressure range. Although the transit time change does not directly measure the change in adsorbed fluid mass at these pressures, reflecting rather the change in elastic modulus, the transit time does directly probe the evolution inside the sample of the negative fluid pressure that drives the variation in the fluid concentration. Thus we expect that the equilibrium time can be meaningfully determined from the ultrasonic velocity data.

The initial rapid increase in transit time, shown in Fig. 11 for measurements immediately after the relative pressure was lowered from 0.6968 to 0.6636 during the desorption branch, was fitted by Eq. (7). This is reasonable since the fluid flow inside the tortuous pore network, once the fluid pressure and density are changed at the surface of the sample, is also a diffusive process, as we show in the following paragraph. At later times, there is evidence of a second, slower mechanism that delays the final approach to equilibrium. Although the microscopic basis of this additional mechanism is not known at present, it may reflect a slow relaxation of the Vycor frame in response to the large change in the negative fluid pressure in the pores. This slower relaxation was fitted by a single exponential decay since this is the simplest phenomenological expression that gives a satisfactory description of the data. The results of fitting these two expressions to the data are shown by the solid curve in Fig. 11; the rapid variation is well described by diffusion, giving a value for the diffusion coefficient of 2.3×10^{-3} cm^2/s, while the exponential fit to the long tail gives a time constant of 370 s.

To see why the change in the fluid pressure diffuses into the filled Vycor when the external pressure is abruptly varied, we consider the following simple argument, which also gives an estimate of the diffusion coefficient. The flow resulting from the pressure change at the surface is governed by Darcy's law

$$\vec{u}=-\frac{k}{\mu}\vec{\nabla}P \ , \tag{8}$$

where $\vec{u}$ is the flow velocity, k is the permeability of the Vycor sample, and μ is the viscosity of hexane. The flow of the hexane must also obey the continuity equation

$$\frac{\partial\rho_H}{\partial t}+\vec{\nabla}\cdot\rho_H\vec{u}=0 \ , \tag{9}$$

where ρ_H is the local value of the density of the liquid hexane in the pore space. By using the chain rule to write the first term in Eq. (9) in terms of the compressibility $\beta_L^{-1}=(1/\rho)(\partial\rho/dP)$, substituting for $\vec{u}$ from Eq. (8) and neglecting the small term involving the product $(\nabla\rho)(\nabla P)$, Eq. (9) can be rewritten as

$$\frac{\partial P}{\partial t}-\frac{k\beta_L}{\mu}\nabla^2P=0 \ . \tag{10}$$

Equation (10) shows that because of compressibility effects, the pressure change diffuses into the sample with a diffusion coefficient $D_P=k\beta_L/\mu$. Using the literature values $k=4.2\times10^{-16}$ cm^2 [28], $\mu=0.0031$ poise [28], and $\beta_L=8.03\times10^9$ $dyne/cm^2$ [19,20], we estimate that $D_P=1.1\times10^{-3}$ cm^2/s. This value is within a factor of 2 of our experimental value, supporting the view that the relaxation observed is due to the rapid "diffusion" of the pressure pulse into the sample. In fact, the numerical discrepancy between the theoretical estimate and our experimental value may simply reflect a difference in the permeability of our sample and that of the one used by Lin *et al.* [28].

On desorption, as the relative pressure is lowered below $p\approx0.48$, corresponding to the onset of the sharp drop in the isotherm on drainage, the behavior of fluid transport in the pores becomes dramatically different. The drainage of fluid from the pores can no longer be described by diffusion; in Fig. 10 there is a gap in the data when $0.48>p>0.45$. The breakdown of equilibration by diffusion is most clearly seen in the variation of the ultrasonic velocity and attenuation with time, both of which are extremely sensitive (because of the interference effects) to the drainage of fluid from the pores. Typical data for the relative transit time are shown in Fig. 12. Although the pressure was maintained constant at $p=0.4799\pm0.0001$ and the sample temperature was maintained constant to better than 0.01 °C, there is no indication over the 100 000 s time interval shown that the distribution of fluid in the pores is approaching equilibrium. Also the evolution of the transit time undergoes fluctuations and undulations as some of the pores suddenly empty in response to minute fluctuations in the local pressure. Thus the fluid distribution is extremely unstable, and in this sense it is very similar to a disordered system about to undergo a phase transition at the critical point. Both systems are extremely sensitive to critical fluctuations. In the case of fluid drainage from Vycor, it appears from our data that this sensitivity to fluctuations persists until virtually all the pores have opened and prevents true equi-

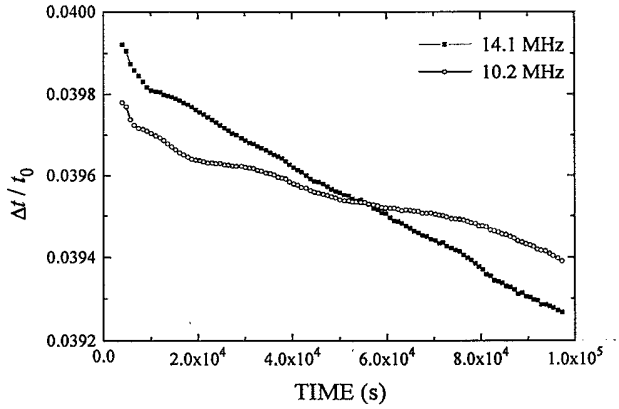

FIG. 12. The variation of the relative transit time measured at two ultrasonic frequencies after the relative pressure was lowered to $p=0.4799$. This illustrates the behavior during the sharp drop in the desorption isotherm, where an equilibrium configuration of fluid in the pores cannot be reached on a time scale of days and the drainage is extremely susceptible to small fluctuations.

librium from being attained at all pressures corresponding to the sharp knee of the desorption isotherm. These data add further support to the analogy between the drainage of the Vycor and invasion percolation; near the percolation threshold, critical behavior is expected, and the dynamics of the Vycor drainage are a direct manifestation of it.

VII. CONCLUSIONS

In this paper, we have studied the adsorption and desorption of hexane in a prototypic porous medium, Vycor. We have combined several techniques to probe the behavior; we measured the amount of fluid adsorbed into the pore space by using either volumetric or gravimetric techniques, we measured the presence of the fluid and vapor in the pore space by determining both the ultrasonic velocity and the attenuation, and we measured the large length scale correlations in the empty pores on draining by using light scattering techniques. The combination of all these methods enables us to develop a consistent picture for the filling and draining of a fluid in Vycor.

We find that on adsorption, the pores of Vycor initially fill uniformly as the ambient vapor pressure is increased. However, once capillary condensation begins, the filling is no longer uniform, but instead the pore space contains regions of vapor bubbles, interspersed with the capillary condensed fluid. Because the vapor is so compressible, the longitudinal modulus of Vycor does not change at all until the pores are almost completely filled with fluid. Thus for *all* pressures at which the pores are partially filled, the longitudinal ultrasonic velocity is sensitive *only* to the change in the sample density, providing an extremely accurate probe of the sorption isotherm. The presence of vapor bubbles also has a dramatic effect on the ultrasonic attenuation, which exhibits a pronounced peak just before the Vycor is completely filled with fluid. We believe that this attenuation peak is caused by viscous dissipation of the fluid as it flows in the pores between the highly compressible bubbles. The sensitivity of these experiments to bubbles in the pores enables us to estimate the size of the largest pore spaces in the Vycor. Using the Kelvin and Laplace equations, these are found to have a radius of about 50 Å.

The behavior on desorption is markedly different. As is often observed in porous materials, the sorption isotherm exhibits pronounced hysteresis, with most of the fluid being desorbed over a very narrow range of pressures that is substantially lower than the pressures at which the fluid is adsorbed. Initially, when the Vycor is fully saturated and the ambient pressure is lowered, only a very small amount of fluid is desorbed from the pores. While this small change in mass should lead to an increase in the ultrasonic velocity over this range; it is instead observed to decrease. This must reflect a decrease in the modulus of the fluid-filled Vycor, which we believe results from the large negative pressures in the pores caused by the interfacial tension of the fluid. As the pressure of the ambient vapor is decreased still further, the amount of fluid adsorbed in the pores of the Vycor decreases very sharply over a very narrow range of pressures. Right when this decrease occurs, the ultrasonic velocity also drops suddenly, until it matches the velocity measured on filling, whereupon no further hysteresis is observed as the pressure of the ambient vapor is decreased further. However, most of the fluid has been drained from the pores by the time the hysteresis has ended. At the same point that the modulus decreases sharply, the ultrasonic attenuation exhibits a sharp peak, indicating the presence of large-scale inhomogeneities in the draining Vycor.

We have elucidated the physics of the drainage process by measuring the small angle light scattering at pressures just before the amount of fluid in the Vycor drops precipitously. At these pressures, the Vycor has begun to scatter light strongly, indicating the formation of the larger structures in the emptying pores. The scattered light exhibits a power-law dependence on the scattering wave vector q, indicating that the structure of the drained pores is fractal, with $d_f \approx 2.6$. The drainage of the Vycor can be described by percolation invasion of the vapor into the pores; the measured fractal dimension is very close to that predicted by models of invasion percolation in three dimensions.

Finally, we also measure the time dependence of both the adsorption and the desorption of the fluid in the pores of the Vycor as the pressure of the ambient vapor is changed. We identify three dramatically different mechanisms by which fluid can enter or leave the porous material as the ambient pressure is changed abruptly to a new value. At low pressures, the fluid transport is dominated by surface diffusion of fluid molecules adsorbed on the pore walls, since the much larger concentration of adsorbed fluid compared with the vapor ensures that Knudsen vapor phase transport is negligibly small. In this regime, the transport is characterized by a surface diffusion coefficient that we find to be of the order of 1×10^{-5} cm^2/s for hexane in Vycor. At high pressures, when the pores are completely filled with liquid, there is a small but measurable flow of fluid due to the change in the fluid density as the negative fluid pressure in the pores changes rapidly in response to the variation in the external vapor pressure. This process is also diffusive and is characterized by a diffusion coefficient that is approximately 200 times larger than that for surface diffusion. Finally, on desorption, there is a third regime in the narrow range of pressures over which the sharp drop in the desorption isotherm occurs; here the desorption process cannot be described by diffusion, and true equilibrium cannot be attained for a macroscopic sample on a time scale of days. Instead, the drainage rate is extremely sensitive to small fluctuations in the local pressure inside the pores, a result that strongly supports our interpretation of the drainage as being analogous to invasion percolation.

The results in this paper illustrate the rich range of phenomena that can occur when a fluid is adsorbed into a porous medium. Because of the randomness of the porous material and because of the large volume of very small pores, neither the adsorption process nor the desorption process is uniform. The presence of vapor

bubbles on adsorption directly reflects the interactions of the fluid with the pore walls; the presence of the long-range, fractal correlations directly reflects the nonuniform connectivity of each pore to the ambient vapor. The knowledge gained by this work is essential in developing a complete understanding of the interactions between a fluid and a porous medium. The effects of the vapor bubbles that persist on adsorption can dramatically alter the propagation and attenuation of sound in the porous medium; the effects of the restricted connectivity and the randomness of the pore space, which result in the long-range, fractal correlations of the draining pores, can dramatically and adversely affect the traditional techniques for measuring the size distribution of the pore space.

ACKNOWLEDGMENTS

J.H.P. wishes to acknowledge the hospitality of Exxon Research and Engineering Co. during a research lave from the University of Manitoba, and support from NSERC of Canada.

[1] S. J. Gregg and K. S. W. Sing, *Adsorption, Surface Area and Porosity* (Academic, London, 1982).
[2] D. Reuthven, *Principles of Adsorption and Adsorption Processes* (Wiley, New York, 1984).
[3] G. Mason, Proc. R. Soc. London, Ser. A **415**, 453 (1988).
[4] J. H. Page, J. Liu, B. Abeles, H. W. Deckman, and D. A. Weitz, Phys. Rev. Lett. **71**, 1216 (1993).
[5] A. J. Liu, D. J. Durian, E. Herbolzheimer, and S. A. Safran, Phys. Rev. Lett. **65**, 1897 (1990).
[6] J. M. Drake and J. Klafter, Phys. Today **43** (5), 46 (1990).
[7] P. Levitz, G. Ehret, S. K. Sinha, and J. M. Drake, J. Phys. Chem. **95**, 6151 (1991).
[8] A. H. Thompson, A. J. Katz, and R. Raschke, Phys. Rev. Lett. **58**, 29 (1987).
[9] D. Wilkinson and J. F. Willemsen, J. Phys. A **16**, 3365 (1983).
[10] C. J. Brinker and G. W. Scherer, *Sol-Gel Science* (Academic, San Diego, 1990).
[11] K. R. McCall and R. A. Guyer, Phys. Rev. B **43**, 808 (1991).
[12] D. H. Evertett, in *The Solid-Gas Interface,* edited by E. A. Flood (Dekker, New York, 1967), Vol. 2, p. 1055.
[13] K. L. Warner and J. R. Beamish, J. Appl. Phys. **63**, 4372 (1988).
[14] S. Brunauer, P. H. Emmett, and E. Teller, J. Am. Chem. Soc. **60**, 309 (1938).
[15] *CRC Handbook of Chemistry and Physics,* edited by R. C. Weast (CRC, Boca Raton, FL, 1983).
[16] Heraeus-Amersil Inc., Technical Brochure No. HAI-9227-3 IM-81, 1981 (unpublished).
[17] M. A. Biot, J. Acoust. Soc. Am. **28**, 168 (1956).
[18] M. A. Biot, J. Acoust. Soc. Am. **28**, 179 (1956).
[19] J. W. Boelhouwer, Physica **34**, 484 (1967).
[20] H. B. Bohidar, J. Appl. Phys. **64**, 1810 (1988).
[21] A. B. Wood, *A Textbook of Sound* (Bell, London, 1941).
[22] E. Herbolzheimer, J. H. Page, and D. A. Weitz (unpublished).
[23] D.H. Trevena, Contemp. Phys. **17**, 109 (1976).
[24] R. J. Speedy, J. Phys. Chem. **86**, 982 (1982).
[25] M. J. Benham, J. C. Cook, J.-C. Li, D. K. Ross, P. L. Hall, and B. Sarkissian, Phys. Rev. B **39**, 633 (1989).
[26] J.-C. Li, D. K. Ross, and M. J. Benham, J. Appl. Crystallogr. **24**, 794 (1991).
[27] J. Crank, *The Mathematics of Diffusion* (Clarendon, Oxford, 1975).
[28] M. Y. Lin, B. Abeles, J. S. Huang, H. E. Stasiewski, and Q. Zhang, Phys. Rev. B **46**, 10 701 (1992).
[29] B. Abeles, L. F. Chen, J. W. Johnson, and J. M. Drake, Isr. J. Chem. **31**, 99 (1991).